

1 Probabilistic calibration of a Greenland Ice Sheet model 2 using spatially-resolved synthetic observations: toward 3 projections of ice mass loss with uncertainties

4
5 **W. Chang¹, P. J. Applegate², M. Haran¹, K. Keller³**

6 [1]{Department of Statistics, Pennsylvania State University, University Park, PA 16802}

7 [2]{Earth and Environmental Systems Institute, Pennsylvania State University, University
8 Park, PA 16802}

9 [3]{Department of Geosciences, Pennsylvania State University, University Park, PA 16802}

10 Correspondence to: W. Chang (wonchang@psu.edu)

11 12 **Abstract**

13 Computer models of ice sheet behavior are important tools for projecting future sea level rise.
14 The simulated modern ice sheets generated by these models differ markedly as input
15 parameters are varied. To ensure accurate ice sheet mass loss projections, these parameters
16 must be constrained using observational data. Which model parameter combinations make
17 sense, given observations? Our method assigns probabilities to parameter combinations based
18 on how well the model reproduces the Greenland Ice Sheet profile. We improve on the
19 previous state of the art by accounting for spatial information, and by carefully sampling the
20 full range of realistic parameter combinations, using statistically rigorous methods.
21 Specifically, we estimate the joint posterior probability density function of model parameters
22 using Gaussian process-based emulation and calibration. This method is an important step
23 toward calibrated probabilistic projections of ice sheet contributions to sea level rise, in that it
24 uses data-model fusion to learn about parameter values. This information can, in turn, be
25 used to make projections while taking into account various sources of uncertainty, including
26 parametric uncertainty, data-model discrepancy, and spatial correlation in the error structure.
27 We demonstrate the utility of our method using a perfect model experiment, which shows that
28 many different parameter combinations can generate similar modern ice sheet profiles. This
29 result suggests that the large divergence of projections from different ice sheet models is

1 partly due to parametric uncertainty. Moreover, our method enables insight into ice sheet
2 processes represented by parameter interactions in the model.

3

4 **1 Introduction**

5 Accurate projections of future sea level rise are important for present-day adaptation
6 decisions. Global mean sea level has risen 0.2-0.3 m over the last two to three centuries (e.g.
7 Church and White, 2006; Jevrejeva et al., 2008), and this rise is expected to continue in the
8 future (Meehl et al., 2007, Alexander et al., 2013; Edwards 2014a, 2014b). A significant
9 fraction of world population and built infrastructure lies near present-day sea level, and these
10 people and resources are at risk from sea level rise. Projections of sea level rise with sound
11 characterization of the associated uncertainties can inform the design of risk management
12 strategies (e.g., Lempert et al., 2012).

13 Here, we focus on the Greenland Ice Sheet component of future sea level rise, as estimated by
14 ice sheet models. Enhanced mass loss from the Greenland Ice Sheet is just one component of
15 overall sea level rise, which also includes contributions from the Antarctic Ice Sheets, small
16 glaciers, thermal expansion of ocean water, and the transfer of water stored on land to the
17 oceans. However, the Greenland Ice Sheet is a large potential contributor to sea level rise,
18 and also a highly uncertain one; if this ice sheet were to melt completely, sea level would rise
19 by about 7 m (Bamber et al., 2001, 2013; Lemke et al., 2007), and both the rate of ice loss and
20 its final magnitude are uncertain (Lenton et al., 2008). Ice sheet models provide internally-
21 consistent representations of the processes that are important to the growth and decay of ice
22 sheets. Although imperfect, such models have been the focus of intense development effort
23 since the fourth Intergovernmental Panel on Climate Change assessment report (e.g.,
24 Bindshadler et al., 2013; Shannon et al., 2013; Edwards et al., 2014a).

25 To yield accurate projections, ice sheet models must be started from an initial condition that
26 resembles the real ice sheet as closely as possible, both in terms of the spatial distribution and
27 flow of ice and the temperature distribution within the ice body. Ice flow is driven primarily
28 by thickness and surface slope (e.g., Alley et al., 2010), and warm ice deforms more easily
29 than cold ice. Similarly, the melt rate of a patch of the ice sheet's surface is strongly sensitive
30 to its elevation (Born and Nisancioglu, 2012). Thus, errors in the initial condition used for ice
31 sheet model projections will lead to inaccuracies in simulated future ice distributions and sea
32 level rise contributions. In practice, all models include simplifications that also affect

1 projection accuracy (e.g., Kirchner et al., 2011), perhaps more than initial condition errors.
2 However, matching the modern ice sheet is a frequently-recurring theme in the literature (e.g.,
3 Ritz et al., 1997; Greve, 1997; Huybrechts, 2002; Stone et al., 2010; Greve et al., 2011;
4 Pollard and DeConto, 2012).

5 The initial condition used in ice sheet models is a function of input parameter values, as well
6 as the spinup method. Because the thermal field within the ice sheet is incompletely known,
7 most modeling studies perform an initialization to bring the simulated ice sheet to a state that
8 is consistent with the present-day climatology (e.g., Stone et al., 2010), climate model output
9 (e.g., Fyke et al., 2011), or climate history estimated from ice cores (e.g., Applegate et al.,
10 2012). Most studies allow the simulated ice sheet's surface topography to evolve during the
11 spinup period; thus, the estimated initial condition usually does not exactly match the
12 observed ice sheet topography (Bamber et al., 2001, 2013). For example, many studies obtain
13 a simulated modern Greenland ice sheet that is larger than expected (e.g. Heimbach et al.,
14 2008; Stone et al., 2010; Robinson et al., 2010; Vizcaino et al., 2010; Greve et al., 2011; cf.
15 Bamber et al., 2001, 2013). Ice sheet models have many uncertain parameters that affect the
16 softness of the ice, the speed of basal sliding, and the intensity of surface melting, among
17 other processes (Ritz et al., 1997; Hebelier et al., 2008; Stone et al., 2010; Fitzgerald et al.,
18 2011; Applegate et al., 2012). Adjusting these parameters changes the simulated modern ice
19 sheet (Stone et al., 2010; Applegate et al., 2012).

20 Despite the importance of achieving a good match between ice sheet model output and the
21 present-day ice geometry, it remains unclear how to use data on the modern ice sheet to assess
22 the relative plausibility of different model runs, in cases where the modeled ice sheet surface
23 topography can evolve freely. The root-mean-squared error (RMSE) is sometimes used for
24 this purpose (e.g., Greve and Otsu, 2007; Stone et al., 2010). However, it is unclear how to
25 translate the RMSE values from a set of model runs into probabilistic projections of ice
26 volume change, as required for sea level studies. Using a probability model that accounts for
27 various uncertainties, as we do here, helps overcome this limitation. Recent work by McNeall
28 et al. (2013) and Gladstone et al. (2012) partly addresses the challenge of identifying
29 appropriate parameter combinations, given observations and a freely-evolving ice sheet
30 model. McNeall et al. (2013) train a statistical emulator (e.g., Sacks et al., 1989; Kennedy
31 and O'Hagan, 2001) to relate input parameter combinations to highly-aggregated metrics
32 describing the Greenland ice sheet's geometry (volume, area, and maximum thickness; Ritz et

1 al., 1997; Stone et al., 2010), using a previously-published ensemble of ice sheet model runs
2 (Stone et al., 2010). The work of McNeall et al. (2013) is groundbreaking in its application of
3 a computationally-efficient statistical emulator to an ice sheet model, allowing estimation of
4 model output at many more design points than would have been possible with the model
5 itself. However, the highly-aggregated metrics used by McNeall et al. (2013) neglect
6 information on the spatial distribution of ice, which might further limit the parameter
7 combinations that agree well with the observed geometry of the modern ice sheet. Moreover,
8 their calibration approach is based on “historical mapping” and does not provide probabilistic
9 projections. Gladstone et al. (2012) proposed a simple, but statistically robust, probabilistic
10 approach for calibrating a flowline model of Pine Island Glacier in West Antarctica, but their
11 approach is applicable only when the ice flow model is computationally cheap and the
12 observational data include only a small number of observations.

13 A second challenge involves characterizing the effects of input parameter choice on the
14 agreement between modeled and observed ice sheets. In an ensemble of Greenland Ice Sheet
15 model runs carried out by Applegate et al. (2012; described below), the parameter
16 combinations that agree well with the modern ice sheet's volume are widely distributed over
17 parameter space, with no easily-discernable structure. This result may arise from
18 uncharacterized interactions among the model parameters. This outcome also has strong
19 implications for model projections of sea level rise from the ice sheet, in that the model runs
20 that agree well with the modern volume constraint give widely diverging sea level rise
21 projections (Applegate et al., 2012).

22 Finally, estimates of future sea level rise require projections of ice volume change with well-
23 characterized uncertainties. Perturbed-parameter ensembles (e.g., Stone et al., 2010;
24 Applegate et al., 2012, Edwards et al., 2014a) represent an important step toward this goal,
25 but the relatively small number of model runs that can be performed in a reasonable time
26 (usually 10^2 - 10^3 ; Stone et al., 2010; Applegate et al., 2012) are insufficient to fully explore
27 model parameter space. As McNeall et al. (2013) demonstrate, statistical emulators help
28 overcome this dimensionality problem; however, some method for assigning plausibility
29 scores to the emulator output is also needed. In a slightly different but relevant context, Little
30 et al. (2013) and Edwards et al. (2014b) use Bayesian model averaging to assign scores to
31 model runs in perturbed-parameter ensembles, but the scores in these methods are essentially

1 based on RMSE for low-dimensional summaries of model output and therefore do not fully
2 account for the spatial information in ice model output.

3 Here, we address these challenges using a Bayesian framework that combines data, models,
4 and prior beliefs about model input parameter values. Like McNeall et al. (2013), we train an
5 emulator on an ensemble of ice sheet model runs. However, we build on their work by using
6 an explicit likelihood function, and by incorporating information from a north-south profile of
7 average ice thicknesses. Specifically, we use a Gaussian process emulator to estimate the first
8 10 principal components of the zonal mean ice thickness profile, following a recent climate
9 model calibration study (Chang et al., 2013). Further, we perform a perfect model experiment
10 to investigate the interactions between input parameters. Our approach recovers the correct
11 parameter values and projected ice volume changes from an "assumed-true" model
12 realization, and the multi-dimensional probability density function displays expected physical
13 interactions (Section 1.2, below). These interactions were not evident from the simple
14 analysis employed by Applegate et al. (2012, their Fig. 1).

15 The above paragraphs discuss the case in which the ice sheet model is free to evolve to the
16 state that is most consistent with the selected parameter combination, the bedrock topography
17 and the climate (whether steady or varying). In such studies, parameters such as the basal
18 sliding coefficient are held constant over the geographic area of the ice sheet. However, a
19 number of recent studies (e.g., Gillet-Chaulet et al., 2012; Quiquet et al., 2012; Goelzer et al.,
20 2013; Shannon et al., 2013; Edwards et al., 2014b) have used an alternative approach in
21 which the spatially-distributed basal sliding coefficients and/or surface mass balance fields
22 are tuned so that the ice sheet model matches the observed modern geometry. This approach
23 has several advantages; the simulated modern ice sheet is guaranteed to match the observed
24 modern one, and the estimated basal sliding coefficients vary spatially, as is almost certainly
25 the case for the real ice sheet. However, such studies are silent on interactions between
26 parameters besides the basal sliding coefficient and surface mass balance, as we investigate
27 here.

28 The paper proceeds as follows. In the remainder of the Introduction, we describe the
29 ensemble that we use to train the emulator. In Section 2, we outline our method for using a
30 Gaussian process emulator to estimate the principal components of the zonally-averaged ice
31 thicknesses, and the setup of our perfect model experiment. Section 3 presents the results of

1 the perfect model experiment. In Section 4, we conclude by pointing out the implications of
2 our work, as well as its limitations and potential directions for future research.

3 **1.1 The ensemble**

4 We train our emulator with a 100-member perturbed-parameter ensemble described in
5 Applegate et al. (2012). This ensemble uses the three-dimensional ice sheet model
6 SICOPOLIS (Greve, 1997; Greve et al., 2011). Each model run spans the period from
7 125,000 years ago (125 ka BP) to 3500, driven by surface temperature and sea level histories
8 derived from geologic data (Imbrie et al., 1984; Dansgaard et al., 1993; Johnsen et al., 1997)
9 and forced into the future with an asymptotic warming to ~ 5 °C above present values.
10 SICOPOLIS is a shallow ice-approximation model, meaning that it neglects longitudinal
11 stresses within the ice body (Kirchner et al., 2011). Like most ice sheet models, it also
12 includes many simplifications in calculating the surface mass balance, notably through its use
13 of the positive degree-day method for relating surface temperatures to melting (Braithwaite,
14 1995; Calov and Greve, 2005; van der Berg et al., 2011). These simplifications improve
15 SICOPOLIS' computational efficiency relative to higher-order or full-Stokes models (e.g.,
16 Seddik et al., 2012), allowing it to be run repeatedly over 10^5 -yr time scales.

17 The parameter combinations in the Applegate et al. (2012) ensemble were chosen by Latin
18 hypercube sampling (McKay et al., 1979), following the earlier work of Stone et al. (2010).
19 Latin hypercube sampling distributes points throughout parameter space more efficiently than
20 Monte Carlo methods (Urban and Fricker, 2010). In their experiment, Applegate et al. (2012)
21 varied the ice flow enhancement factor, the ice and snow positive degree-day factors, the
22 geothermal heat flux, and the basal sliding factor (Ritz et al., 1997; cf. Stone et al., 2010;
23 Fitzgerald et al., 2011). These parameters control the softness of ice, the rapidity with which
24 the ice sheet's surface lowers at a given temperature, the amount of heat that enters the base of
25 the ice sheet, and the speed of sliding at a given stress (see Applegate et al., 2012, for an
26 explanation of how each parameter affects model behavior).

27 McNeall et al. (2013) trained their emulator using a perturbed-parameter ensemble of ice
28 sheet model runs published by Stone et al. (2010). Key differences between the Applegate et
29 al. (2012) ensemble and the Stone et al. (2010) ensemble involve the parameters varied in the
30 ensembles and the processes included in the simulations. Stone et al. (2010) varied the lapse
31 rate instead of the basal sliding factor adjusted by Applegate et al. (2012). The model used by

1 Stone et al. (2010; Glimmer v. 1.0.4; see Rutt et al., 2009) neglects basal sliding, a process
2 included in the SICOPOLIS runs presented by Applegate et al. (2012).

3 The results presented by Applegate et al. (2012) suggest that widely diverging ice sheet model
4 parameter values yield comparable modern ice sheets, but substantially different sea level rise
5 projections. Applegate et al. (2012) assessed the plausibility of their model runs by
6 comparing the simulated ice volumes in 2005 to the estimated modern ice volume (Bamber et
7 al., 2001; Lemke et al., 2007); those runs that yielded modern ice volumes within 10% of the
8 estimated value were kept. These plausible runs yielded a range of future sea level rise
9 projections that was ~75% of the median estimate.

10 Moreover, the parameter combinations that agree well with the modern ice volume constraint
11 are widely distributed over parameter space. With the exception of the ice positive degree-
12 day factor, where only values less than $\sim 15 \text{ mm day}^{-1} \text{ }^{\circ}\text{C}^{-1}$ satisfy the ice volume constraint,
13 no pattern emerges from the distribution of the successful runs through parameter space.
14 McNeall et al. (2013) make a similar point using their own results. Statistically, this inability
15 to learn about the plausibility of various parameter combinations given observations is termed
16 an "identifiability problem."

17 **1.2 Expected interactions among model input parameters**

18 The apparently-structureless distribution of successful runs through parameter space
19 (Applegate et al., 2012, their Fig. 1) may stem from interactions among the parameters. The
20 parameters can be loosely grouped into those that control the ice sheet's surface mass balance
21 (the ice and snow positive degree-day factors) and those that control ice movement (the ice
22 flow enhancement factor, the basal sliding factor, and the geothermal heat flux). Either group
23 of parameters can cause mass loss from the ice sheet to be high or low, given fixed values of
24 the parameters in the other group. For example, a high ice positive degree-day factor should
25 be associated with a low snow positive degree-day factor to produce the same amount of melt
26 as a model run with more moderate values of both parameters. This interaction is bounded,
27 however, because the maximum snow positive degree-day factor is much lower than the
28 maximum value for ice; also, at the peak of the ablation season, there is no snow left on the
29 lower parts of the ice sheet, so the ice positive degree-day factor dominates over part of the
30 year. Similarly, the same ice velocities can be produced by either a high flow enhancement
31 factor and a low basal sliding factor, or the reverse. Basal sliding can be a much faster

1 process than ice flow, so this parameter interaction is also bounded. However, basal sliding
2 operates only where the bed is thawed, and the geothermal heat flux likely controls the
3 fraction of the bed that is above the pressure melting point.

4 The relatively small number of design points in the ensemble presented by Applegate et al.
5 (2012) hinders mapping of the interactions among parameters over their five-dimensional
6 space. Coherent mapping requires many more design points, but performing these additional
7 runs with the full ice sheet model is impractical because of the model's high computational
8 cost. This problem suggests a need for a computationally efficient emulator to fill the gaps in
9 parameter space between the existing model runs.

10

11 **2 Methods**

12 As described above, our goals are 1) to present a method for quantifying the agreement
13 between ice sheet model output and observations that incorporates spatial information, 2) to
14 characterize the interactions among input parameters, and 3) to produce illustrative
15 projections of sea level rise from the Greenland Ice Sheet based on synthetic data. In this
16 section, we provide an outline of our methods for achieving these goals; fuller descriptions
17 appear in Chang et al. (2013) and in the Supporting Information.

18 We accomplish goal #1 through constructing a statistical model that results in a likelihood
19 function. This statistical model compares ice sheet model output and observations to evaluate
20 the plausibility of a vector of model input parameter values $\boldsymbol{\theta}$ while accounting for systematic
21 discrepancies between the model output and the observations. The likelihood function for the
22 ice thickness observations, denoted by \mathbf{Z} , is based on the additive model

$$23 \quad \mathbf{Z} = \mathbf{Y}(\boldsymbol{\theta}) + \boldsymbol{\delta} + \boldsymbol{\varepsilon}, \quad (1)$$

24 where $\mathbf{Y}(\boldsymbol{\theta})$ is the ice thickness output from SICOPOLIS model at the vector of input
25 parameter values $\boldsymbol{\theta}$, $\boldsymbol{\delta}$ is the discrepancy between model output and observations caused by
26 structural problems in the model, and $\boldsymbol{\varepsilon}$ is independently- and identically-distributed
27 observational noise. To achieve goal #2, we perform a "leave-one-out" perfect model
28 experiment with a Gaussian process emulator, a computationally-cheap surrogate for the full

1 ice sheet model. As described above, the model output $\mathbf{Y}(\boldsymbol{\theta})$ is available only at a relatively
2 small number of points in parameter space, and therefore it is necessary to build an emulator
3 that approximates the model output $\mathbf{Y}(\boldsymbol{\theta})$ at any given $\boldsymbol{\theta}$.

4 Direct emulation of the full two-dimensional ice thickness grid is prohibitively expensive, due
5 to (i) the cost of performing operations on large covariance matrices (see the Supplementary
6 Information and Chang et al., 2013, for details) and (ii) the need to model spatial processes
7 that contain many zeros, which poses non-trivial computational and inferential challenges. To
8 mitigate these problems, we take the mean of each row in the ice thickness grid, thereby
9 obtaining a 264-element vector of zonally-averaged ice thicknesses for each ice sheet model
10 run. We then apply principal component analysis to these mean ice thickness vectors. The
11 magnitudes of the first 10 principal components suffice to recover the mean ice thickness
12 vectors. Because the principal components are uncorrelated, we can construct a separate
13 emulator for the magnitude of each principal component. Our emulator consists of all these
14 independent Gaussian processes. Although our emulator operates in the principal component
15 space, we can reconstruct the ice thickness profile that corresponds to the emulated principal
16 components (see the Supporting Information for details). Note that our likelihood formulation
17 automatically penalizes the components with lower explained variation.

18 Next, we train the emulator on all but one of the model runs. We refer to the output
19 (specifically, the zonal mean ice thickness profile and the ice volume change projection) from
20 this left-out model run as our "assumed truth." We examined the robustness of our methods
21 by successively leaving out each model run in turn and repeating our analysis; see the
22 Supplementary Information.

23 Before using the mean ice thickness profile from our assumed-true model run in our perfect
24 model experiment, we contaminate it with spatially-correlated errors. These errors reflect the
25 discrepancies that we would expect to see between model output and data in a "real"
26 calibration experiment, due to missing or parameterized processes in the model. In particular,
27 we use spatially-correlated errors with a moderate magnitude (standard deviation of 50 m)
28 and a large-scale spatial trend to represent a situation in which (i) the ice sheet model has
29 reasonable skill in reproducing the observed spatial pattern of modern ice thickness, and (ii)
30 the discrepancy pattern is notably different from patterns generated by the ice sheet model and
31 is therefore statistically identifiable (see the Supplementary Information for more details).

1 Note that any probabilistic calibration method, including our approach, can be uninformative
2 if condition (i) is violated, or subject to serious bias if condition (ii) is violated.

3 We then use Markov chain Monte Carlo (MCMC) to estimate the joint posterior probability
4 distribution over the five-dimensional input parameter space. MCMC is a well-established
5 (Hastings, 1970), but complex, statistical technique; Brooks et al. (2011) provide a book-
6 length treatment. Briefly, the Metropolis-Hastings algorithm used in MCMC constructs a
7 sequence of parameter combinations, each of which is chosen randomly from the region of
8 parameter space surrounding the last point. Candidate parameter combinations are accepted if
9 the posterior probability of the new point is greater than at the previous one, or with a certain
10 probability determined by the Metropolis-Hastings acceptance ratio otherwise. If the
11 candidate point is rejected, another candidate point is chosen at random according to a
12 proposal distribution. Consistent with McNeall et al. (2013), we match the emulator estimates
13 to assumed-true model output instead of observed ice thickness values (Bamber et al., 2001,
14 2013) because a perfect model experiment is more suitable to achieve our main objectives,
15 studying and demonstrating the performance of our probabilistic calibration method. The
16 candidate points that are retained by the MCMC algorithm approximate the posterior
17 probability distribution of the input parameter space. The candidate points from this algorithm
18 therefore reflect various characteristics of the posterior distribution, including the marginal
19 distributions of each of the parameters separately and their joint distributions. Hence, we can
20 use MCMC to summarize what we have learned about the parameters from the model and
21 observations while accounting for various uncertainties and prior information.

22 Finally, to achieve goal #3, we use a separate Gaussian process emulator to interpolate
23 between the ice volume change projections from all the model runs in the original ensemble
24 (Applegate et al., 2012), except the assumed-true realization. When applied to the sample of
25 the model input parameters that we obtained from Markov chain Monte Carlo, this emulator
26 yields a sample of ice volume changes, and thus sea level rise contributions, between 2005
27 and 2100. We then use kernel density estimation to compute the probability density of the
28 projected sea level rise contributions. It should be noted that these projections are based on
29 synthetic data (not real observations), and do not represent "real" projections of Greenland Ice
30 Sheet mass loss over this century.

31

1 **3 Results**

2 Besides helping to diagnose interactions among ice sheet model parameters, our perfect
3 model experiment allows us to test our overall procedure. We carry out several checks.

4 1) If the trained emulator is given the parameter settings from the left-out model realization, it
5 should produce a close approximation to the actual output from that realization.

6 2) The maximum of the multidimensional posterior probability function from our Markov
7 chain Monte Carlo analysis should lie close to the parameter settings from the left-out model
8 realization.

9 3) The mode of the probability density function of ice loss projections should be close to the
10 ice loss projection from the assumed-true model realization.

11 As detailed below, our methods pass all three of these checks.

12 Aggregating the ice thicknesses to their zonal means allows easy visual comparison of
13 different emulator-estimated ice thickness vectors to the assumed-true model realization
14 (black curve, Fig. 1). The emulator, as trained on 99 of the model realizations from the
15 Applegate et al. (2012) ensemble, successfully recovers the ice thicknesses from the left-out
16 model realization (Fig. 2) when given the parameter combination for that left-out model
17 realization as input. Differences between the assumed-true and emulated zonally-averaged
18 ice thickness vectors are minor. Thus, our methods pass check #1, above.

19 Similarly, the conditional posterior density functions (Fig. 3) have maxima near the assumed-
20 true parameter values. Parameter combinations yielding zonally-averaged ice thickness curves
21 that lie close to the assumed-true model realization (e.g., the red curve in Fig. 1) are more
22 likely (more probable based on the posterior distribution) than those with curves that lie
23 farther from the assumed-true values (blue and green curves in Fig. 1). We do not expect that
24 the modes of the marginal posterior density functions (Fig. 4b) will fall exactly at the
25 assumed-true parameter values, because summing over one or more dimensions often moves
26 the marginal mode away from the maximum of the multidimensional probability density
27 function. In any case, the maximum posterior probability is close to the assumed-true
28 parameter combination. Thus, our methods pass check #2, above. Some of the two-
29 dimensional marginal probability density functions (Fig. 4b) show multiple modes and bands
30 of high probability extending across the two-dimensional fields; we discuss the significance
31 of these features below.

1 For comparison, we also produced scatterplots of parameter combinations as projected onto
2 two-dimensional slices through the five-dimensional parameter space (Fig. 4a), following
3 Applegate et al. (2012, their Fig. 1). As in Applegate et al. (2012), the "successful" design
4 points show no clustering around the assumed-true parameter values, except for the ice PDD
5 factor.

6 Our method also successfully recovers the ice volume loss produced by the assumed-true
7 model realization (Fig. 5; see also Figs. S3, S4), reflected by the close correspondence
8 between the mode of the probability density function produced by our methods and the
9 vertical black line. Thus, our methods pass check #3, listed above. As previously noted,
10 these projections are based on synthetic data; they are not "real" projections of Greenland Ice
11 Sheet mass loss. For comparison, we also applied the windowing approach used by
12 Applegate et al. (2012) to the model runs and the synthetic observation. The 95% probable
13 interval produced by our methods is much smaller than that estimated by computing the 2.5th
14 and the 97.5th percentiles of the synthetic volume change values selected by the 10% volume
15 filter used in Applegate et al. (2012). This reflects the utility of spatial information and our
16 probabilistic calibration approach in reducing projection uncertainties comparing to the
17 windowing approach in Applegate et al. (2012).

18 The prior density for the ice volume loss was constructed by assuming that all 99 design
19 points used to train our emulator are equally likely. Interestingly, a uniform prior for the
20 input parameters results in a skewed and multimodal prior distribution for the volume loss,
21 indicating that the function that maps input parameters to projected ice volume changes is
22 highly non-linear and not smooth. These characteristics also cause a small offset between the
23 assumed-true projection and the mode of the posterior density. The marginal plots for the
24 volume loss projection surfaces are shown in Figure S1 in the supporting material.

25

26 **4 Discussion**

27 As explained above, our goals for this work were to identify an objective function for
28 matching ice sheet models to spatially-distributed data (especially ice thicknesses), map
29 interactions among model input parameters, and develop methods for projecting future ice
30 sheet mass loss, with well-characterized uncertainties. We demonstrated that our emulator
31 reproduces a vector of zonally-averaged ice thicknesses from a given model run when trained
32 on other members from the same ensemble (Fig. 2). We further showed that the emulator can

1 recover the appropriate parameter combinations for an assumed-true model realization in a
2 perfect model experiment (Figs. 3, 4b). Finally, we produced illustrative projections of
3 Greenland Ice Sheet mass loss, based on synthetic data (Fig. 5; see also Figs. S3, S4). As
4 noted above, our projections are for illustration only, and do not represent "real" projections
5 of future Greenland Ice Sheet mass loss.

6 The utility of our approach becomes clear in comparing the marginal posterior probability
7 density functions (Fig. 4a) and projections (red probability density functions and boxplots in
8 Figs. 5, S3, and S4) to results from simpler methods (Fig. 4b; blue boxplots in Figs. 5, S3, and
9 S4; Applegate et al., 2012). In Figure 4b, there are distinct modes in the marginal densities,
10 indicating regions of parameter space that are more consistent with the assumed truth. These
11 modes are absent in the simpler graphic (Fig. 4a). Similarly, the 95% probable interval of sea
12 level rise contributions is narrower using our methods than if a simple windowing approach is
13 applied (Fig. 5; see also Figs. S3, S4). Our results also show the importance of including the
14 discrepancy term (δ in Eqn. 1) for recovering the appropriate parameter settings in our perfect
15 model experiments (Fig. S2). If we leave this discrepancy term out, the marginal posterior
16 density functions for each parameter clearly miss the true values.

17 The parameter interactions identified in this experiment are generally consistent with intuition
18 (see Section 1.2 for descriptions of anticipated parameter interactions). Figure 4 shows
19 inclined bands of high marginal posterior probability in the ice positive degree-day vs. snow
20 positive degree-day, geothermal heat flux vs. ice flow factor, and basal sliding factor vs. flow
21 factor panels. As expected, there are tradeoffs among each of these parameter pairs; for
22 example, a low ice positive degree-day factor must be combined with a high snow positive
23 degree-day factor to produce a reasonable match to the assumed truth. Somewhat surprisingly,
24 the tradeoff between the geothermal heat flux and the ice flow factor is much stronger than
25 that between the geothermal heat flux and the basal sliding factor. The geothermal heat flux
26 affects both ice deformation (which is temperature-sensitive) and basal sliding (which
27 operates only where there is liquid water at the ice-bed interface). We hypothesize that the
28 geothermal heat flux has a stronger effect on ice flow than basal sliding because ice
29 deformation happens over a much larger fraction of the ice sheet's basal area than does sliding.
30 Multiple modes appear in the two-dimensional marginal density plots (Fig. 4), implying that
31 standard methods for tuning of ice sheet models may converge to "non-optimal" parameter
32 combinations. Ice sheet models are commonly tuned by manually adjusting one parameter at

1 a time until the simulated modern ice sheet resembles the real one (e.g., Greve et al., 2011).
2 This procedure is an informal variant of so-called gradient descent methods, which search for
3 optimal matches between models and data by moving down a continuous surface defined by
4 the model's input parameters, the objective function, and the data. If the surface has multiple
5 "peaks" (i.e. regions of parameter space that are more plausible, given observations, than their
6 surroundings), gradient descent methods can converge to a point which produces a better
7 match to the data than any adjacent point, but is nevertheless far from the "best" parameter
8 combination.

9 This problem may partly explain the wide variation in projections of sea level rise from the
10 ice sheets, as made with state-of-the-art ice sheet models. Two recent intercomparison
11 projects, SeaRISE and ice2sea (Bindschadler et al. 2013; Shannon et al., 2013; Edwards et al.,
12 2014a) used a variety of ice sheet models to project future ice sheet contributions to sea level
13 rise. The two projects used different groups of ice sheet models and different methods for
14 spinning up the participating models. The results of one of these projects shows strong
15 divergence among the results from different models (Bindschadler et al. 2013), whereas the
16 other project's projections agree more closely (Shannon et al. 2013; Edwards et al., 2014a).
17 The multiple modes in our posterior two-dimensional density plots (Fig. 4) suggest that some
18 of the divergence among models, for example in the SeaRISE project (Bindschadler et al.,
19 2013), may be due to differences in model tuning: even if the models had similar structures
20 and reproduced the modern ice sheet topography and ice thicknesses equally well, we would
21 still expect their future projections to diverge because of differences in input parameter choice.
22 Our leave-one-out cross-validation shows that the results presented here are consistent across
23 all possible 100 synthetic truths. The prediction interval for the ice volume changes in Fig 5
24 achieves the nominal coverage when the synthetic truth yields a modern ice volume that is
25 close to the observed modern ice volume (Fig. S5). The parameter interactions shown in Fig.
26 4 are also consistent across the majority of the synthetic truths (Fig. S6).

27 **4.1 Cautions and future directions**

28 In this paper, we specifically avoid giving "real" projections of future Greenland Ice Sheet
29 volume change, for two reasons. First, we match only a two-dimensional profile of zonally-
30 averaged ice thicknesses from an assumed-true model run, rather than the two-dimensional
31 grid of observed ice thicknesses (Bamber et al., 2001, 2013; see also McNeall et al., 2013).

1 Second, the ensemble of ice sheet model runs (Applegate et al., 2012) that we use to calibrate
2 our emulator has several important limitations, including the relative simplicity of the model
3 used to generate the ensemble and the synthetic climate scenario used to drive the ensemble
4 members into the future. Most importantly, this ensemble's simulated modern ice sheets are
5 generally too thick in the southern part of Greenland and too thin in the northern part of the
6 island (Applegate et al., 2012, their Fig. 7); other studies that allow the ice sheet surface to
7 evolve freely have noted similar difficulties in reproducing the modern ice sheet (e.g., Stone
8 et al., 2010; Greve et al., 2011; Nowicki et al., 2013, their Fig. 2; cf. Edwards et al., 2014a).
9 The long-term goal of this work is to compare ice sheet model runs to actual data, thereby
10 resulting in probabilistic projections of future ice sheet mass loss. To achieve this goal, we
11 plan to expand our method to treat the full, two-dimensional ice thickness grid and take
12 advantage of other spatially-distributed data sets (e.g., surface velocities; Joughin et al. 2010),
13 and to generate new ice sheet model ensembles that overcome the limitations explained above.

14

15 **5 Conclusions**

16 In this paper, we presented an approach for probabilistic calibration of ice sheet models using
17 spatially-resolved ice thickness information. Specifically, we constructed a probability model
18 for assigning posterior probabilities to individual ice sheet model runs, and we used a
19 Gaussian process emulator to interpolate between existing ice sheet model simulations. We
20 reduced the dimensionality of the emulation problem by reducing profiles of mean ice
21 thicknesses to their principal components. Finally, we showed how the posterior probabilities
22 from the model calibration exercise can be used to make projections of future sea level rise
23 from the ice sheets. In a perfect model experiment where the "true" parameter settings and
24 future contributions of the ice sheet to sea level rise are known, our methods successfully
25 recovered these values. The posterior probability density function that resulted from this
26 experiment shows tradeoffs among parameters and multiple modes. The tradeoffs are
27 consistent with physical expectations, whereas the multiple modes may indicate that
28 commonly-applied methods for tuning ice sheet models can lead to calibration errors.

29

30 **Acknowledgements**

1 We thank R. Greve for distributing his ice sheet model SICOPOLIS freely on the Web
2 (<http://sicopolis.greveweb.net/>), and N. Kirchner for help in setting up and using the model.
3 R. Alley and D. Pollard provided helpful comments on a draft of the manuscript. This work
4 was partially supported by the US Department of Energy, Office of Science, Biological and
5 Environmental Research Program, Integrated Assessment Program, Grant No. DE-
6 SC0005171; by the US National Science Foundation through the Network for Sustainable
7 Climate Risk Management (SCRiM) under NSF cooperative agreement GEO-1240507; and
8 by the Penn State Center for Climate Risk Management. Any opinions, findings, and
9 conclusions expressed in this work are those of the authors, and do not necessarily reflect the
10 views of the National Science Foundation or the Department of Energy. Supplementary
11 material related to this article is available online at [http://www.geosci-model-dev-](http://www.geosci-model-dev-discuss.net/7/1905/2014/gmdd-7-1905-2014-supplement.pdf)
12 [discuss.net/7/1905/2014/](http://www.geosci-model-dev-discuss.net/7/1905/2014/gmdd-7-1905-2014-supplement.pdf) gmdd-7-1905-2014-supplement.pdf.

13 **Author Contributions**

14 WC designed the emulator, carried out the analyses, and wrote the first draft of the
15 Supplementary Information. PJA wrote the first draft of the body text and supplied the
16 previously-published ice sheet model runs (available online at
17 <http://bolin.su.se/data/Applegate-2011>). WC, PJA, MH, and KK jointly designed the research
18 and edited the paper text.

19

1 **References**

- 2 Alley, R. B., Andrews, J. T., Brigham-Grette, J., Clarke, G. K. C., Cuffey, K. M., Fitzpatrick,
3 J. J., Funder, S., Marshall, S. J., Miller, G. H., Mitrovica, J. X., Muhs, D. R., Otto-Bliesner, B.
4 L., Polyak, L., and White, J. W. C.: History of the Greenland Ice Sheet: paleoclimatic insights,
5 *Quaternary Sci. Rev.*, 29, 1728–1756, 2010.
- 6 Applegate, P. J., Kirchner, N., Stone, E. J., Keller, K., and Greve, R.: An assessment of key
7 model parametric uncertainties in projections of Greenland Ice Sheet behavior, *The*
8 *Cryosphere*, 6, 589–606, doi:10.5194/tc-6-589-2012, 2012.
- 9 Alexander, L. V., Allen, S. K., Bindoff, N. L., Bron, F. M., Church, J. A., Cubasch, U., Emori,
10 S., Forster, P., Friedlingstein, P., Gillett, N., Gregory, J. M., Hartmann, D. L., Jansen, E.,
11 Kirtman, B., Knutti, R., Kanikicharla, K. K., Lemke, P., Marotzke, J., Masson-Delmotte, V.,
12 Meehl, G. A., Mokhov, I. I., Piao, S., Plattner, G. K., Dahe, Q., Ramaswamy, V., Randall, D.,
13 Rhein, M., Rojas, M., Sabine, C., Shindell, D., Stocker, T. F., Talley, L. D., Vaughan, D. G.
14 and Xie, S. P. (2013). *Climate Change 2013: The Physical Science Basis: Contribution of*
15 *Working Group I to the Fifth Assessment Report of the Intergovernmental Panel on Climate*
16 *Change*. IPCC, Cambridge University Press, Cambridge.
- 17 Bamber, J. L., Layberry, R. L., and Gogineni, S. P.: A new ice thickness and bed data set for
18 the Greenland ice sheet 1. Measurement, data reduction, and errors, *J. Geophys. Res.*, 106,
19 33773–33780, 2001.
- 20 Bamber, J. L., Griggs, J. A., Hurkmans, R. T. W. L., Dowdeswell, J. A., Gogineni, S. P.,
21 Howat, I., Mouginot, J., Paden, J., Palmer, S., Rignot, E., and Steinhage, D.: A new bed
22 elevation dataset for Greenland, *The Cryosphere*, 7, 499–510, doi:10.5194/tc-7-499-2013,
23 2013.
- 24 Bindschadler, R. A., Nowicki, S., Abe-Ouchi, A., Aschwanden, A., Choi, H., Fastook,
25 J., Granzow, G., Greve, R., Gutowski, G., Herzfeld, U., Jackson, C., Johnson, J., Khroulev, C.,
26 Levermann, A., Lipscomb, W. H., Martin, M. A., Morlighem, M., Parizek, B. R., Pollard, D.,
27 Price, S. F., Ren, D., Saito, F., Sato, T., Seddik, H., Seroussi, H., Takahashi, K., Walker, R.,
28 and Wang, W. L.: Ice-sheet model sensitivities to environmental forcing and their use in
29 projecting future sea level (the SeaRise project), *J. Glaciol.*, 59, 195–224, 2013.
- 30 Born, A. and Nisancioglu, K. H.: Melting of Northern Greenland during the last
31 interglaciation, *The Cryosphere*, 6, 1239–1250, doi:10.5194/tc-6-1239-2012, 2012.

1 Braithwaite, R. J.: Positive degree-day factors for ablation on the Greenland ice sheet studied
2 by energy-balance modelling, *J. Glaciol.*, 41, 153–160, 1995.

3 Brooks, S., Gelman, A., Jones, G., and Meng, X.-L. (Eds.): *Handbook of Markov Chain*
4 *Monte Carlo*, Chapman and Hall/CRC, 619 pp., 2011.

5 Calov, R. and Greve, R.: A semi-analytical solution for the positive degree-day model with
6 stochastic temperature variations, *J. Glaciol.*, 51, 173–175, 2005.

7 Chang, W., Haran, M., Olson, R., and Keller, K.: Fast dimension-reduced climate model
8 calibration, *Ann. Appl. Stat.*, accepted, 2014.

9 Church, J. A. and White, N. J.: A 20th century acceleration in global sea-level rise, *Geophys.*
10 *Res. Lett.*, 33, L01602, doi:10.1029/2005GL024826, 2006.

11 Cuffey, K. M. and Kavanaugh, J. L.: How nonlinear is the creep deformation of polar ice? A
12 new field assessment, *Geology*, 39, 1027–1030, 2011.

13 Edwards, TL, Fettweis, X, Gagliardini, O, Gillet-Chaulet, F, Goelzer, H, Gregory, J, Hoffman,
14 M, Huybrechts, P, Payne, AJ, Perego, M, Price, S, Quiquet, A & Ritz, C: Effect of uncertainty
15 in surface mass balance–elevation feedback on projections of the future sea level contribution
16 of the Greenland ice sheet. *The Cryosphere*, 8, 195-208 doi:10.5194/tc-8-195-2014, 2014a

17 Edwards, TL, Fettweis, X, Gagliardini, O, Gillet-Chaulet, F, Goelzer, H, Gregory, J, Hoffman,
18 M, Huybrechts, P, Payne, AJ, Perego, M, Price, S, Quiquet, A & Ritz, C: Probabilistic
19 parameterisation of the surface mass balance elevation feedback in regional climate model
20 simulations of the Greenland ice sheet. *The Cryosphere*, 8, 181-194 doi:10.5194/tc-8-181-
21 2014, 2014b

22 Fitzgerald, P. W., Bamber, J. L., Ridley, J. K., and Rougier, J. C.: Exploration of parametric
23 uncertainty in a surface mass balance model applied to the Greenland ice sheet, *J. Geophys.*
24 *Res.*, 117, F01021, doi:10.1029/2011JF002067, 2012.

25 Gillet-Chaulet, F., Gagliardini, O., Seddik, H., Nodet, M., Durand, G., Ritz, C., Zwinger, T.,
26 Greve, R., and Vaughan, D. G.: Greenland ice sheet contribution to sea-level rise from a new-
27 generation ice-sheet model, *The Cryosphere*, 6, 1561-1576, doi:10.5194/tc-6-1561-2012,
28 2012.

29 Goelzer, H., Huybrechts, P., Fürst, J. J., Nick, F. M., Andersen, M. L., Edwards, T. L.,
30 Fettweis, X., Payne, A. J., and Shannon, S.: Sensitivity of Greenland ice sheet projections to

1 model formulations, *Journal of Glaciology*, 59 (216), 1-17,
2 <http://dx.doi.org/10.3189/2013JoG12J182>, 2013.

3 Fyke, J. G., Weaver, A. J., Pollard, D., Eby, M., Carter, L., and Mackintosh, A.: A new
4 coupled ice sheet/climate model: description and sensitivity to model physics under Eemian,
5 Last Glacial Maximum, late Holocene and modern climate conditions, *Geosci. Model Dev.*, 4,
6 117–136, doi:10.5194/gmd-4-117-2011, 2011.

7 Greve, R.: Application of a polythermal three-dimensional ice sheet model to the Greenland
8 Ice Sheet: response to steady-state and transient climate scenarios, *J. Climate*, 10, 901–918,
9 1997.

10 Greve, R. and Otsu, S.: The effect of the north-east ice stream on the Greenland ice sheet in
11 changing climates, *The Cryosphere Discuss.*, 1, 41–76, doi:10.5194/tcd-1-41-2007, 2007.

12 Greve, R., Saito, F., and Abe-Ouchi, A.: Initial results of the SeaRISE numerical experiments
13 with the models SICOPOLIS and IcIES for the Greenland Ice Sheet, *Ann. Glaciol.*, 52, 23–30,
14 2011.

15 Hastings, W. K.: Monte Carlo sampling methods using Markov chains and their applications,
16 *Biometrika*, 57, 97–109, 1970.

17 Hebel, F., Purves, R. S., and Jamieson, S. S. R.: The impact of parametric uncertainty and
18 topographic error in ice-sheet modelling, *J. Glaciol.*, 54, 899–919, 2008.

19 Heimbach, P. and Bugnion, V.: Greenland ice-sheet volume sensitivity to basal, surface and
20 initial conditions derived from an adjoint model, *Ann. Glaciol.*, 50, 67–80, 2009.

21 Huybrechts, P.: Sea-level changes at the LGM from ice-dynamic reconstructions of the
22 Greenland and Antarctic ice sheets during the glacial period, *Quaternary Sci. Rev.*, 21, 203–
23 231, 2002.

24 Jevrejeva, S., Moore, J. C., Grinsted, A., and Woodworth, P. L.: Recent global sea level
25 acceleration started over 200 years ago?, *Geophys. Res. Lett.*, 35, L08715,
26 doi:10.1029/2008GL033611, 2008.

27 Joughin, I., Smith, B. E., Howat, I. M., Scambos, T., and Moon, T.: Greenland flow
28 variability from ice-sheet-wide velocity mapping, *J. Glaciol.*, 56, 415–430, 2010. Kennedy, M.
29 C. and O’Hagan, A.: Bayesian calibration of computer models, *J. R. Statist. Soc. B*, 63, 425–
30 464, 2001.

1 Kirchner, N., Hutter, K., Jakobsson, M., and Gyllencreutz, R.: Capabilities and limitations of
2 numerical ice sheet models: a discussion for Earth-scientists and modelers, *Quaternary Sci.*
3 *Rev.*, 30, 3691–3704, 2011.

4 Lemke, P., Ren, J., Alley, R. B., Allison, I., Carrasco, J., Flato, G., Fujii, Y., Kaser, G., Mote,
5 P., Thomas, R. H., and Zhang, T.: Observations: changes in snow, ice, and frozen ground,
6 edited by: Solomon, S., Qin, D., Manning, M., Chen, Z., Marquis, M., Averyt, K. B., Tignor,
7 M., and Miller, H. L., Cambridge University Press, Cambridge, 2007.

8 Lempert, R., Sriver, R. L., and Keller, K.: Characterizing uncertain sea level rise projections
9 to support investment decisions, California Energy Commission Report CEC-500-2012-056,
10 2012.

11 Lenton, T. M., Held, H., Kriegler, E., Hall, J. W., Lucht, W., Rahmstorf, S., and
12 Schnellhuber, H. J.: Tipping elements in the Earth’s climate system, *P. Natl. Acad. Sci. USA*,
13 105, 1786–1793, 2008.

14 Little, C. M., Oppenheimer, M., Urban, N. M.: Upper bounds on twenty-first-century
15 Antarctic ice loss assessed using a probabilistic framework, *Nature Climate Change* 3, 654–
16 659, doi:10.1038/nclimate1845, 2013

17 McKay, M. D., Beckman, R. J., and Conover, W. J.: A comparison of three methods for
18 selecting values of input variables in the analysis of output from a computer code,
19 *Technometrics*, 21, 239–245, 1979.

20 McNeall, D. J., Challenor, P. G., Gattiker, J. R., and Stone, E. J.: The potential of an
21 observational data set for calibration of a computationally expensive computer model, *Geosci.*
22 *Model Dev.*, 6, 1715-1728, doi:10.5194/gmd-6-1715-2013, 2013.

23 Meehl, G. A., Stocker, T. F., Collins, W. D., Friedlingstein, P., Gaye, A. T., Gregory, J. M.,
24 Kitoh, A., Knutti, R., Murphy, J. M., Noda, A., Raper, S. C. B., Watterson, I. G., Weaver, A.
25 J., and Zhao, Z.-C.: Global climate projections, edited by: Solomon, S., Qin, D., Manning, M.,
26 Chen, Z., Marquis, M., Averyt, K. B., Tignor, M., and Miller, H. L., Cambridge University
27 Press, Cambridge, 2007.

28 Nowicki, S., Bindshadler, R. A., Abe-Ouchi, A., Aschwanden, A., Bueler, E., Choi, H.,
29 Fastook, J., Granzow, G., Greve, R., Gutowski, G., Herzfeld, U., Jackson, C., Johnson, J.,
30 Khroulev, C., Larour, E., Levermann, A., Lipscomb, W. H., Martin, M. A., Morlighem, M.,
31 Parizek, B. R., Pollard, D., Price, S. F., Ren, D., Rignot, E., Saito, F., Sato, T., Seddik, H.,

1 Seroussi, H., Takahashi, K., Walker, R., and Wang, W. L.: Insights into spatial sensitivities of
2 ice mass response to environmental change from the SeaRISE ice sheet modeling project II:
3 Greenland, *J. Geophys. Res.-Earth*, 118, 1025–1044, doi:10.1002/jgrf.20076, 2013.

4 Pollard, D. and DeConto, R. M.: A simple inverse method for the distribution of basal sliding
5 coefficients under ice sheets, applied to Antarctica, *The Cryosphere*, 6, 953–971,
6 doi:10.5194/tc-6-953-2012, 2012.

7 Quiquet, A., Punge, H. J., Ritz, C., Fettweis, X., Gallée, H., Kageyama, M., Krinner, G., Salas
8 y Méliá, D., and Sjolte, J.: Sensitivity of a Greenland ice sheet model to atmospheric forcing
9 fields, *The Cryosphere*, 6, 999–1018, doi:10.5194/tc-6-999-2012, 2012.

10 Ritz, C., Fabre, A., and Letreguilly, A.: Sensitivity of a Greenland Ice Sheet model to ice flow
11 and ablation parameters: consequences for the evolution through the last climatic cycle, *Clim.*
12 *Dynam.*, 13, 11–24, 1997.

13 Robinson, A., Calov, R., and Ganopolski, A.: An efficient regional energy-moisture balance
14 model for simulation of the Greenland Ice Sheet response to climate change, *The Cryosphere*,
15 4, 129–144, doi:10.5194/tc-4-129-2010, 2010.

16 Rutt, I. C., Hagdorn, M., Hulton, N. R. J., and Payne, A. J.: The Glimmer community ice-
17 sheet model, *J. Geophys. Res.-Earth*, 114, F02004, doi:10.1029/2008JF001015, 2009.

18 Sacks, J., Welch, W. J., Mitchell, T. J., and Wynn, H. P.: Design and analysis of computer
19 experiments (with discussion), *J. Stat. Sci.*, 4, 409–423, 1989.

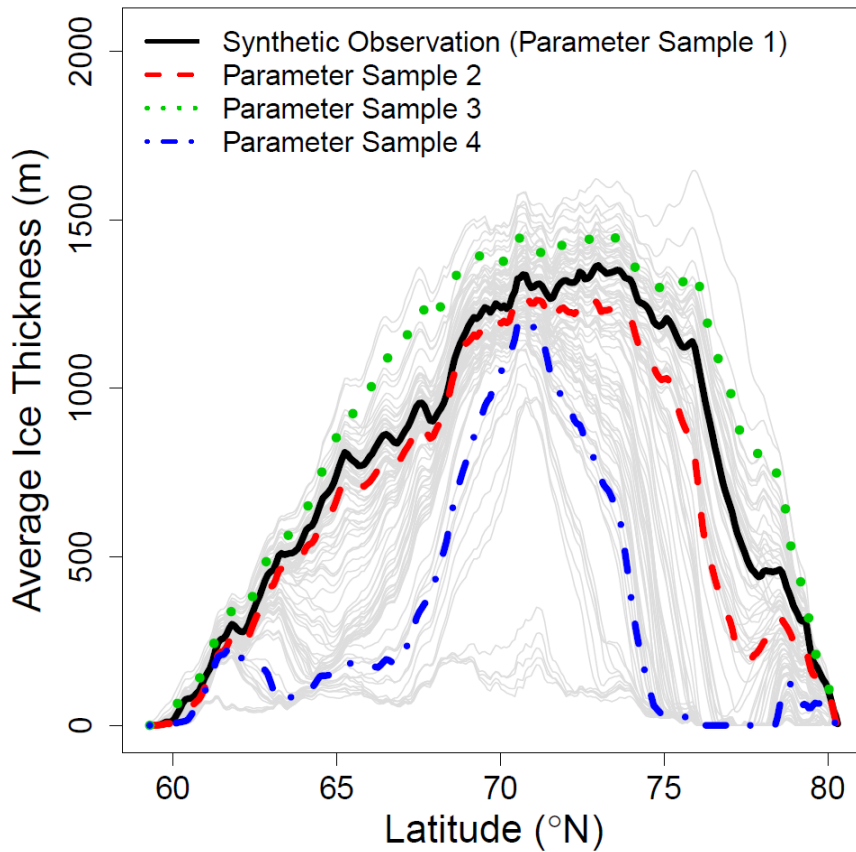
20 Seddik, H., Greve, R., Zwinger, T., Gillet-Chaulet, F., and Gagliardini, O.: Simulations of the
21 Greenland ice sheet 100 years into the future with the full Stokes model Elmer/Ice, *J. Glaciol.*,
22 58, 427–440, 2012.

23 Stone, E. J., Lunt, D. J., Rutt, I. C., and Hanna, E.: Investigating the sensitivity of numerical
24 model simulations of the modern state of the Greenland ice-sheet and its future response to
25 climate change, *The Cryosphere*, 4, 397–417, doi:10.5194/tc-4-397-2010, 2010.

26 Urban, N. M. and Fricker, T. E.: A comparison of Latin hypercube and grid ensemble designs
27 for the multivariate emulation of an Earth system model, *Comput. Geosci.*, 36, 746–755, 2010.

28 van der Berg, W. J., van den Broeke, M., Ettema, J., van Meijgaard, E., and Kaspar, F.:
29 Significant contribution of insolation to Eemian melting of the Greenland ice sheet, *Nat.*
30 *Geosci.*, 4, 679–683, 2011.

1 Vizcaino, M., Mikolajewicz, U., Jungclaus, J., and Schurgers, G.: Climate modification by
2 future ice sheet changes and consequences for ice sheet mass balance, *Clim. Dynam.*, 34,
3 301– 324, 2010.
4



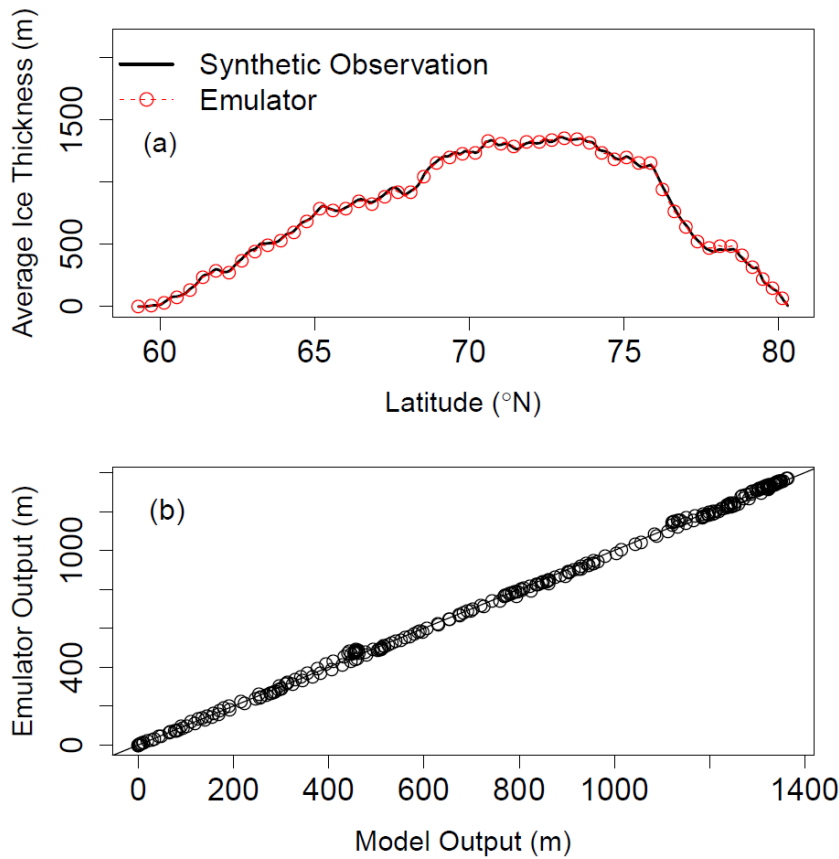
1

2

3 **Figure 1.** Profiles of zonal mean ice thicknesses from four different evaluations of the ice
 4 sheet model SICOPOLIS (Greve, 1997; Greve et al., 2011). The solid black curve represents
 5 model run #67 from Applegate et al. (2012), which we take to be the synthetic truth for our
 6 perfect model experiments. The other curves represent examples of model runs used to
 7 construct the emulator: one run produces a zonal mean ice thickness curve similar to the
 8 synthetic observations (dashed red curve), another is generally too thick (dotted green curve),
 9 and a third is generally too thin (dot-dashed blue curve). As expected, our probability model
 10 assigns a greater posterior probability to the model run represented by the red curve than to
 11 the model runs represented by the blue and green curves. All the other model runs that are not
 12 highlighted above are represented as grey curves.

13

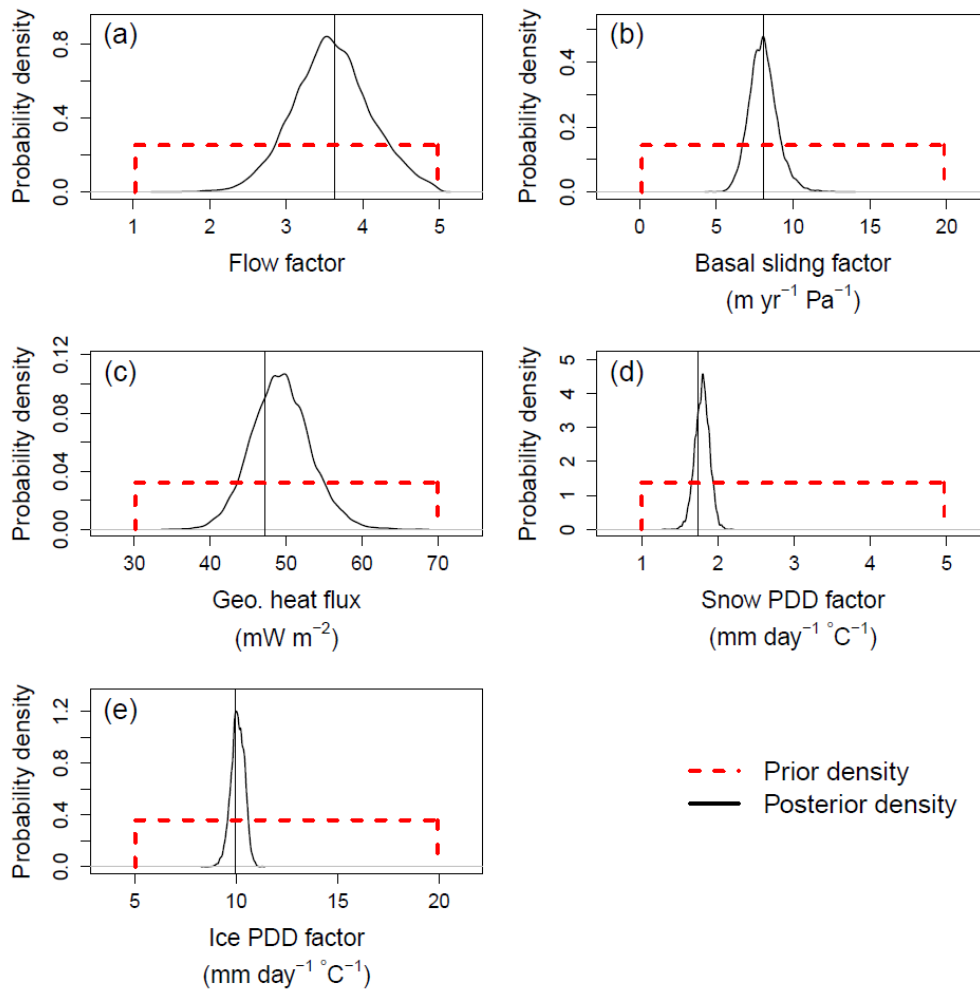
14



1

2

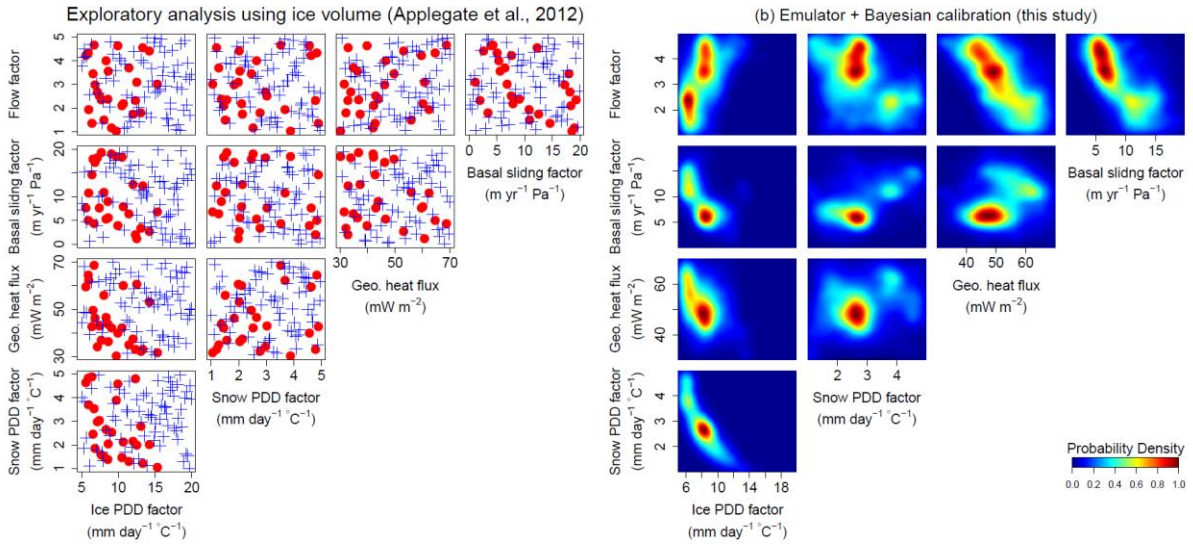
3 **Figure 2.** Comparison of zonal mean ice thickness transects from the assumed-true model
 4 run (#67 from Applegate et al., 2012) and that generated by the trained emulator at the same
 5 parameter combination as used in the assumed-true model run. In the top panel, the assumed-
 6 true profile is shown by a solid black line, and the emulator output is shown by a dashed red
 7 curve with circles. In the lower panel, each point stands for an individual latitude location.
 8 The red circles in the top panel fall almost exactly on top of the black curve, and the points in
 9 the lower panel fall almost exactly on a 1:1 line connecting the lower left and upper right
 10 corners of the plot. Thus, the emulator successfully recovers the ice thicknesses from an
 11 assumed-true model realization when trained on the other model runs from the same
 12 ensemble.



1

2

3 **Figure 3.** Prior (dashed red curves) and posterior (solid black curves) probability density
 4 functions of each input parameter, assuming that all the other parameters are held fixed at
 5 their assumed-true values. The vertical lines indicate the assumed-true values of the
 6 individual parameters.

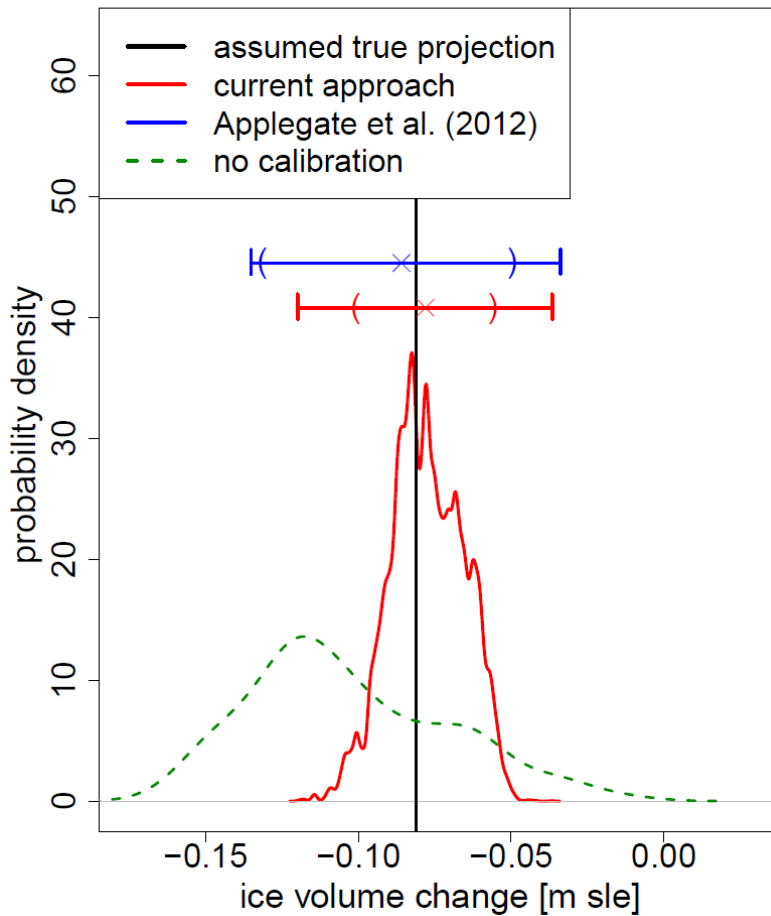


1

2

3 **Figure 4.** Comparison between an exploratory data analysis, following Applegate et al.
 4 (2012), and the results of our probabilistic calibration. (a) Scatterplots of parameter settings
 5 used to train the emulator, as projected onto two-dimensional marginal spaces. Red dots,
 6 parameter settings resulting in simulated modern ice volumes within 10% of the synthetic
 7 truth (model run #67 of Applegate et al. 2012); blue crosses, parameter settings that yield ice
 8 volumes more than 10% larger or smaller than the synthetic truth. (b) Two-dimensional
 9 marginal posterior densities of all pairs of input parameters. Several of the marginal posterior
 10 density maps show inclined bands of higher probability, indicating interactions among
 11 parameters; other panels show multiple modes, representing potential "traps" for tuning of ice
 12 sheet models using simpler methods. See text for discussion.

Illustrative projections based on synthetic data



1

2

3 **Figure 5.** Illustrative (not "real") ice volume change projections between 2005 and 2100,
4 based on three different methods: i) the prior density of the input parameters (dashed green
5 line); ii) parameter settings that pass the 10% ice volume filter used by Applegate et al. (2012)
6 (solid blue line); and iii) the posterior density computed by our calibration approach (solid red
7 line). The vertical line shows the ice volume change projection for the assumed-true
8 parameter setting. The horizontal lines and the parentheses on them represent the range and
9 the 95% prediction intervals, respectively; the crosses indicate the median projection from
10 each method. The width of the 95% projection interval from our methods is narrower than if
11 simpler methods are applied (blue boxplot; Applegate et al., 2012). Similar results are
12 obtained if different model runs from the ensemble are left out (see Figs. S3 and S4). See text
13 for discussion. m sle, meters of sea level equivalent.

14